

Received August 12, 2021, accepted September 8, 2021, date of publication October 13, 2021, date of current version October 26, 2021.

Digital Object Identifier 10.1109/ACCESS.2021.3119756

Design of a Wide-Beam Microstrip Array Antenna for Automotive Radar Application

XINYAN YANG¹ AND XIANFENG LIU²

¹Glasgow College, University of Electronic Science and Technology of China (UESTC), Chengdu 611731, China

²School of Electronic Science and Engineering, University of Electronic Science and Technology of China (UESTC), Chengdu, Sichuan 611731, China

Corresponding author: Xianfeng Liu (xianfengliu@uestc.edu.cn)

This work was supported by the Foundation for Innovative Research Group of the National Natural Science Foundation of China under Grant 61721001.

ABSTRACT In this paper, a novel wide-beam microstrip patch array antenna is proposed for automotive radar applications. Different from the regular wide-beam antenna, which is designed to achieve the wide-beam unit radiation performance, the proposed array antenna introduces the coupled-mode technology of the microstrip antenna to design an inclined unit radiation beam. The array elements are arranged alternately and in opposite phases so that the unit radiation beams alternately point to two sides of the array. The wide-beam feature and the high gain performance are realized simultaneously by the array characteristics. The excellent beamwidth and antenna gain performance enable enormous application potential in automotive radar. An 8-unit prototype working at 24 GHz is designed and fabricated for automotive radar applications. Measured results show that the special design scheme extends the horizontal-plane half-power beamwidth (HPBW) to 140°, and the maximum antenna gain is over 10.5 dBi.

INDEX TERMS Array antenna, microstrip antenna, wide-beamwidth, coupled-mode, automotive radar.

I. INTRODUCTION

With the rapid development of wireless communication systems, the application of electronic products is increasingly widening: the field of automotive electronics is no exception. The vision for fully autonomous vehicles equipped with active safety and comfort systems is steadily advancing. While fully autonomous vehicles are the ultimate goal, an even more pressing requirement has been the need for advanced driver assistance systems, which can provide crucial situational information to assist driver operation. All kinds of sensors are indispensable in order to obtain all kinds of situational information, and automotive radar is one of the key technologies [1]–[3]. The high-gain needle beam antennas are nearly always adopted in long-range and middle-range radar applications [4]–[6], while the short-range radar (SRR) system always requires a wide horizontal angular coverage. Hence, the antennas for SRR systems are often linear array models with a fan radiation beam [7], [8].

Due to the features of simple structure, light weight, and easy integration, microstrip antennas have become the most common choice for automotive radar. The beamwidth of a

typical microstrip antenna array for SRR systems is approximately 70° - 80° [8], [9], which does not meet the requirement of wide horizontal angular coverage for SRR radar application. The typical SRR systems require the antenna horizontal beamwidth to be greater than 130° to ensure that the radar system can cover a sufficient range. Naturally, how to broaden the beamwidth of microstrip antennas has become the research focus of practitioners.

Enhancing the horizontal beamwidth of the unit is the easiest method to imagine and the most widely used approach to broaden the horizontal beamwidth of a microstrip antenna vertical line array. The radiation of a typical microstrip antenna element can be equivalent to that of a two-unit magnetic current array, while the array factor can improve the antenna directivity, yet reduce the antenna beamwidth. Hence multipole antenna [10], [11] and single magnetic dipole [12], [13] are often adopted in the widebeam antenna. Designing the half-mode microstrip antenna by shorting via array is a typical implementation scheme. In [13], by constructing a single magnetic current radiation microstrip antenna model, the beamwidth of the element was even extended to over 170°. Based on the same design concept, the wire antenna unit reported in [14] also realized a decent beamwidth performance of 150°. However, this method

The associate editor coordinating the review of this manuscript and approving it for publication was Davide Comite¹.

usually causes severe deterioration of the cross-polarization level of the H-plane. The H-plane cross-polarization levels of the designs in both [13] and [14] are more than -10 dB. Although the high cross-polarization can be suppressed by shorting the two end edges of the patch [15], this will increase the size of the patch and is thus restricted in line array application. A vertical linear array is exactly what the SRR systems requires.

In addition, introducing the parasitic structure to the microstrip antenna is another method to enhance beamwidth performance. In [16], the parasitic loop improved the beamwidth performance of the microstrip antenna to 130° . Two I-shaped parasitic elements were placed next to the main patch to establish a three-element subarray as introduced in [17] for beamwidth enhancement. The current directions of the parasitic elements are opposite to that of the main patch, leading to extending the beamwidth to 138° . The method of introducing the parasitic structure can indeed expand the horizontal plane beamwidth to partially satisfy the requirements of SRR systems. However, introducing the parasitic structure will increase the width of the microstrip unit, which is not suitable for applications in systems with two or more receiving antennas. The multi-receiving system requires the distance between the adjacent receiving antennas to be less than $1/2\lambda_0$ (λ_0 is the free-space wavelength at working frequency), otherwise, the angle resolution will exhibit a multi-solution error.

In this paper, beamwidth enhancement is reconsidered for array perspective, instead of considering expanding the beam-width of the antenna unit as in other literature. The coupled-mode patch antenna is introduced as the element of the proposed array antenna. The configuration of coupled-mode patch antenna is similar to a regular patch antenna, but shorting vias are designed at the center, which can adjust the even-mode resonant frequency to close to that of the odd-mode resonant frequency [18], [19]. The coupled modes enable the phase changing with frequency at the two radiating slots. The antenna, then, behaves similar to an array of two radiating elements with controllable phases, and thus the radiation beam can bias from the broadsiding direction [20]. The unit structure shares the benefits of a typical microstrip antenna: simplicity, compact size, and low cost.

The units in the proposed array antenna are arranged alternately and symmetrically in the array and are excited alternately in antiphase. Hence, the radiation beams of elements can alternately bias to the two sides of the array, and the synthesized radiation pattern of the array can achieve a wider beamwidth in the plane orthogonal to the array placement. Meanwhile, the array feature offers a high antenna gain performance. Based on the design concept, an 8-unit prototype working at 24 GHz is designed and fabricated for automotive radar applications. The horizontal-plane half-power beamwidth (HPBW) of the prototype is extended to 140° with an antenna gain over 10 dBi, which can meet the wide-beam requirement of the SRR system.

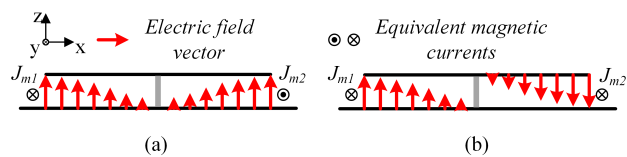


FIGURE 1. E-field distribution of the microstrip patch antenna. (a) Even-mode and (b) Odd-mode.

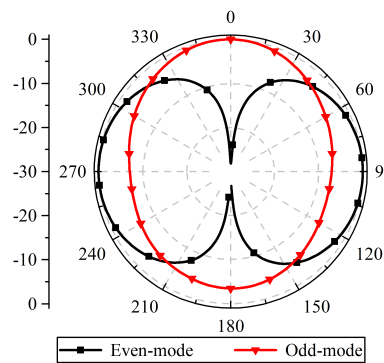


FIGURE 2. E-plane radiation patterns of the even-mode and odd-mode.

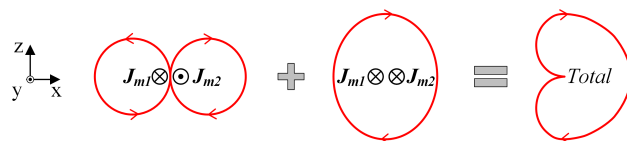


FIGURE 3. Synthesis of the radiation patterns of the even and odd modes.

II. PRINCIPLE OF OPERATION

A. COUPLED-MODE MICROSTRIP ANTENNA UNIT

The even-mode and odd-mode are two typical resonance modes for a microstrip antenna. The radiation of even-mode can be equivalent to a pair of magnetic currents with anti-phase [Fig. 1(a)], while they are in-phase for the odd mode [Fig. 1(b)]. By setting the distance of the two magnetic currents to be $0.2\lambda_0 - 0.3\lambda_0$, the radiation pattern of the even-mode shows a figure- ∞ shape in the E-plane (xoz-plane), while a quasi-omnidirectional figure-0 pattern can be generated by the odd-mode (Fig. 2). If the two modes of the microstrip patch have a proper relationship of amplitude and phase, their radiation fields can be synthesised as shown in Fig. 3. Specifically, the figure- ∞ pattern of the even-mode and the figure-0 pattern of the odd-mode can synthesize a heart-shape unidirectional endfire radiation, which is the fundamental of the titling beam of coupled-mode microstrip antenna.

By adding the shorting vias on the microstrip antenna, the even-mode and odd-mode can resonate at similar frequencies. A back-fed coupled-modes microstrip antenna is shown as Fig. 4. The unit is designed based on a Taconic RF-35 substrate with a dielectric constant of 3.5 and a thickness of 0.25 mm, and the detailed structure parameters are listed in Table 1. Compared with the typical microstrip

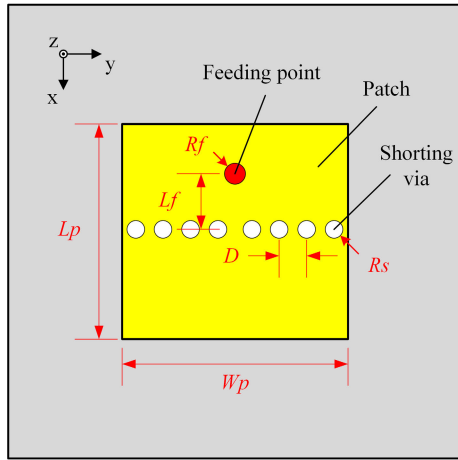
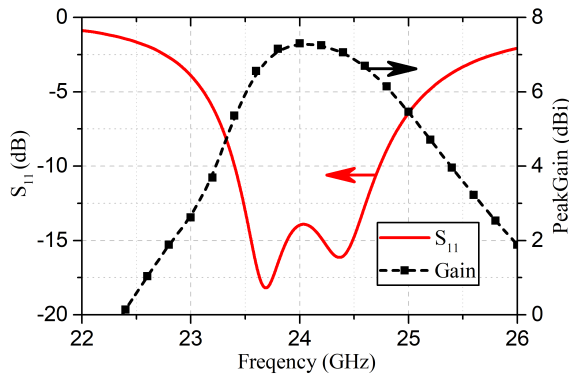
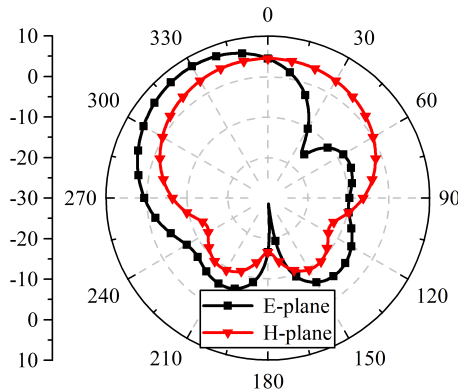


FIGURE 4. The structure of the coupled-mode unit.



(a)



(b)

FIGURE 5. Simulated results of the coupled-mode microstrip antenna. (a) S_{11} and gain, (b) radiation patterns.

antenna working in TM_{10} -mode (odd mode), the obvious difference is that an additional shoring vias array divide the patch into two parts. The shorting vias can force the resonant frequency of the even-mode closing to that of the odd-mode and achieve the special dual-mode resonant model. As shown in Fig. 5(a), two obvious S_{11} notches can be noticed and the S_{11} notch at the lower frequency end is introduced by the

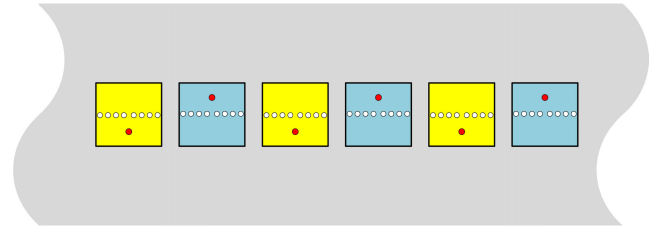


FIGURE 6. The proposed array layout for the wide-beam performance.

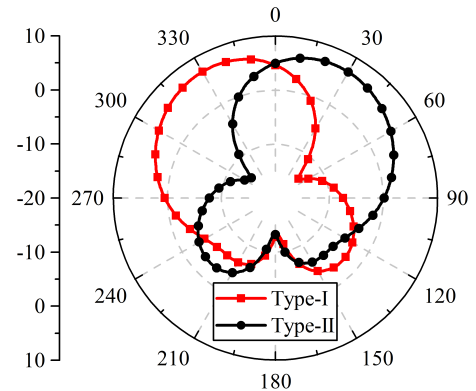


FIGURE 7. The E-plane radiation patterns for the two type units.

TABLE 1. Optimized design parameters of coupled-mode unit.

Parameters	L_p	W_p	L_f	R_f	D	R_s
Value (mm)	3.22	3.3	0.65	0.15	0.4	0.15
Value (λ_0)	0.26	0.26	0.052	0.012	0.032	0.012

even-mode of the microstrip patch, while the S_{11} notch at the higher frequency end belongs to the original odd-mode. Both the even-mode and odd-mode of the microstrip antenna can be simultaneously excited at the middle frequency band. Just like the previous analysis, when the two modes are excited at the same time, a unidirectional end-fire radiation pattern can be realized. Due to the fringe electric field radiation of the limited ground plane, the ideal end-fire radiation like the analysis (Fig. 3) cannot be achieved. Instead, a tilted radiation beam is realized. As shown in Fig. 5(b), the main beam of the simulated E-plane (xoz -plane) radiation pattern is shifted to the feed point direction in xoz -plane.

B. WIDE-BEAM MECHANISM

Based on the special radiation scheme of the coupled-mode microstrip antenna, a special array arrangement can be considered. As shown in Fig. 6, the coupled-mode units are arranged alternately on the H-plane, so the units can be divided into two types. The yellow patches in Fig. 6 are type-I, and the blue patches are classified as type-II. Obviously, the E-plane radiation beam of the type-I units and type-II units, as shown in Fig. 7, will tilt to the two sides of broadsiding direction, respectively. Because of the alternately

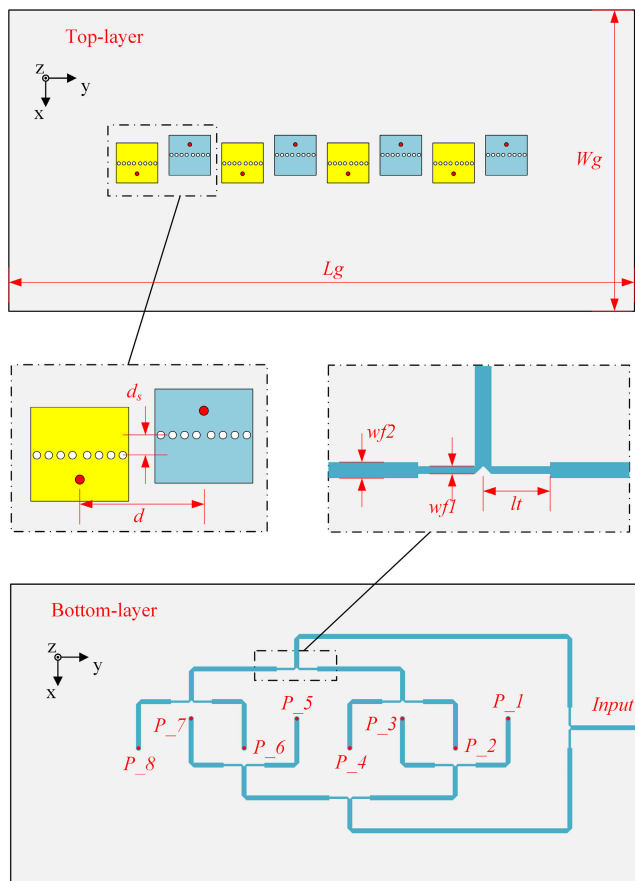


FIGURE 8. The structure of the proposed 24 GHz wide-beam array antenna. $L_g = 60$, $W_g = 30$, $d = 5.2$, $d_s = 1.2$, $wf_1 = 0.28$, $wf_2 = 0.53$, $l_t = 1.95$, unit: mm.

arranged units, alternative anti-phased excitation in the array is need so that these elements can radiation the same polarization. Hence when the two unit types are excited with equal amplitude and inverse phase, a wide-beam array radiation pattern can be synthesized. Moreover, both the compact unit size ($0.26 \lambda_0 \times 0.26 \lambda_0$) and the standard broadsiding radiation of the H-plane indict the feasibility of this array arrangement.

III. WIDE-BEAM ARRAY ANTENNA DESIGN

A. ARRAY ARRANGEMENT

Based on the proposed wide-beam radiation synthesis scheme, an 8-unit wide-beam array antenna is designed at 24 GHz for automotive radar application. The array antenna structure is shown as Fig. 8 and the unit is the same as in Fig. 4. The proposed wide-beam array antenna is constructed with two layers of substrate and three copper layers. The unit patches are designed on the top layer, the feeding network is designed on the bottom layer, and the middle copper layer is the shared ground plane of the microstrip antenna and the microstrip feeding network.

The space between two adjacent units (d) is 5.2 mm, which is less than the half space wavelength of 24 GHz. The shrinking unit spacing is designed for an acceptable

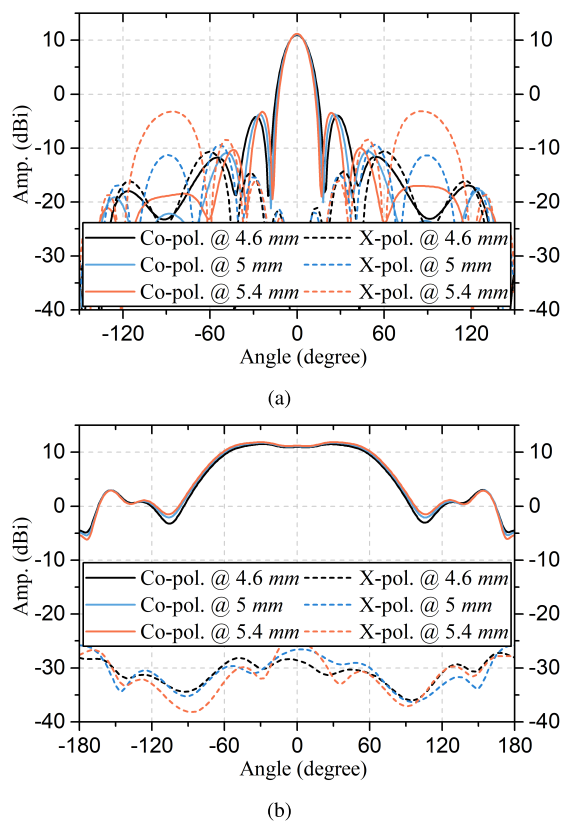


FIGURE 9. The effect of the element distance d on the (a) H-plane and (b) E-plane radiation pattern.

cross-polarization performance. As shown in Fig. 9(a), the H-plane cross-polarization will deteriorate with increasing unit spacing, especially in the direction parallel to the substrate. However, a slightly higher broadsiding gain is also achievable with increasing unit spacing, and so a unit spacing of approximately 5-5.2 mm is suitable for both the antenna gain and the cross-polarization level. The unit spacing is a critical factor for the H-plane cross-polarization level, while it exerts basically no impact on E-plane radiation. As shown in Fig. 9(b), the variety of the parameter d exerts no essential effect on the E-plane wide-beam radiation. The simulated results show that the E-plane beamwidth of the 8-unit array is approximately 135° , which is excellent performance for a planar array antenna.

From the top layer shown in Fig. 8, it can be noticed that the geometric centers of the array units are not distributed on a straight line but are alternately distributed on the two sides of the central axis. This can be attributed to the reason that the radiation phase center of the coupled-mode antenna is not at the geometric center. The alternately staggered distribution can cause the phase centers of each unit to lie on a straight line, which is beneficial to the formation of wide-beam radiation. As shown in Fig. 10, the E-plane wide-beam radiation is sensitive to different offset values (d_s). When d_s is positive, the yellow units are offset in the positive direction of the x -axis compared to the blue units (Fig. 8), and an obvious

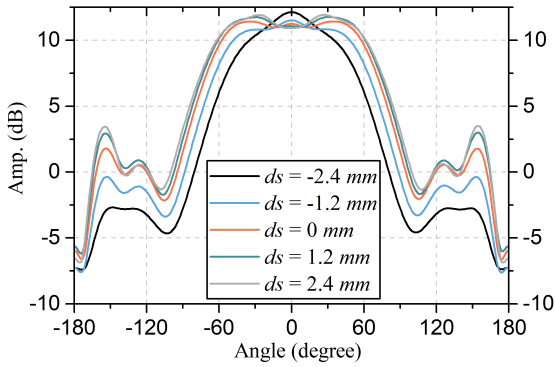


FIGURE 10. The effect of ds on the E-plane radiation pattern.

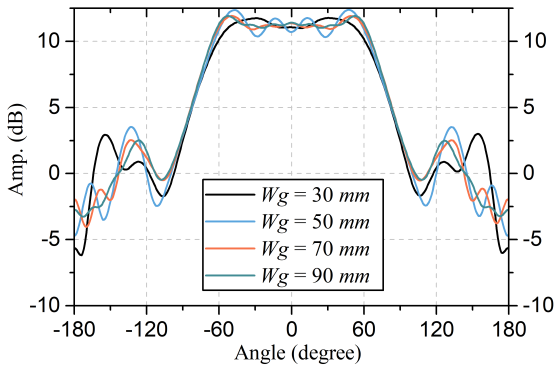


FIGURE 11. The effect of the width of groundplane (W_g) on E-plane radiation pattern.

wide-beam radiation pattern with the flat top feature can be realized (Fig. 10). However, when ds is negative, which means that the yellow units are offset in the negative direction of the x -axis compared to the blue units (Fig. 8), the E-plane beamwidth is narrowed and the broadsiding gain is higher. The optimized value of ds is 1.2 mm, which can take into account wide-beam performance and compact array structure at the same time.

For planar wide-beam antennas, the influence of the edge radiation of the ground plane on the radiation characteristics is inevitable, so the ground plane size parameters are discussed first. As shown in Fig. 11, as the width of the ground plane changes, the wide-beam radiation performance in the E-plane will produce certain fluctuations, while the wide-beam and flat-top radiation characteristics can remain unchanged. Therefore, increasing the size of the ground plane has no essential effect on wide-beam radiation.

Because of the compact arrangement of the array antenna, the coupling between the adjacent units is serious and the active- S_{11} for every unit must be considered. As shown in Fig. 12, a decent overlapped bandwidth can be noticed for every element, since the two frequency points of even-mode and odd-mode are merged into one frequency band.

B. FEEDING NETWORK

Due to the special excitation requirement of the proposed array antenna, alternately inverse phase excitation with equal

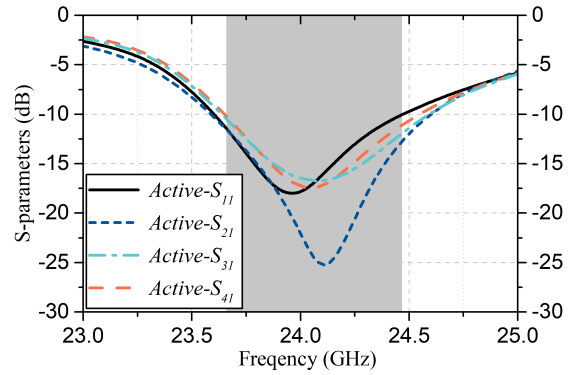


FIGURE 12. The magnitude of active reflection coefficients of the 8-element array.

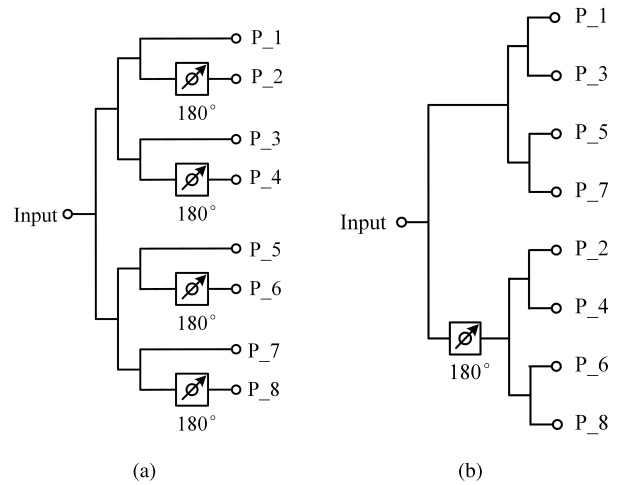
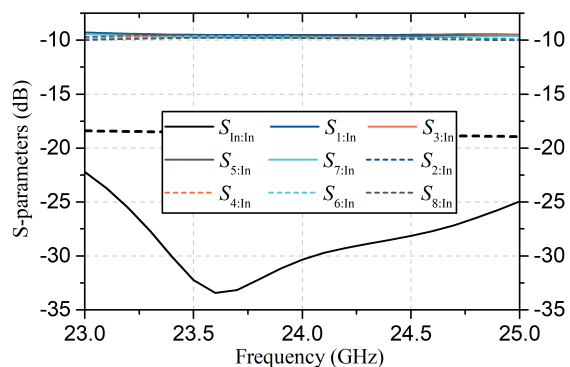


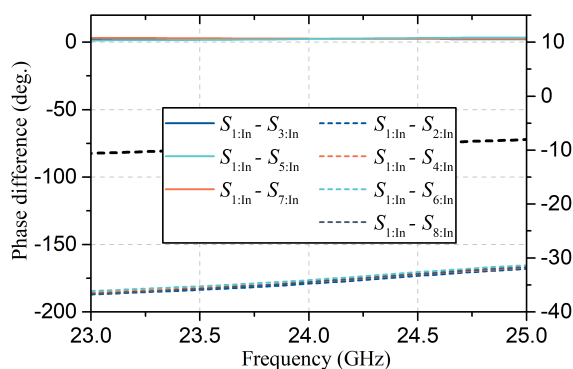
FIGURE 13. The topology models of the 1-8 feeding network. (a) type-I and (b) type-II.

amplitude is necessary. To realize the special excitation model, there are two different feeding network topologies, as shown in Fig. 13. One is designing the 180° phase shift structure between the feeding network and the feeding port (Fig. 13(a)), while the other includes the 180° phase shift structure inset between the first order and second order power divider (Fig. 13(b)). In this design, in order to simplify layout complexity, the second feeding network scheme is chosen and realized by microstrip line network. As shown in the bottom layer in Fig. 8, the 180° phase shift structure is realized by an extended microstrip line.

The simulated results of the 1-8 feeding network are shown in Fig. 14. Good amplitude consistency can be noticed. The amplitude difference of the transmission coefficient between the input port and the 8 output port is less than 0.3 dB, and the average transmission coefficient is approximately -9.6 dB, which means that the insertion loss of the feeding network is approximately 0.6 dB. The phase fluctuation is less than $\pm 5^\circ$, and the alternately inverse phase excitation is also verified.



(a)



(b)

FIGURE 14. Simulated S-parameters of the 1-8 feeding network. (a) magnitude and (b) phase difference.

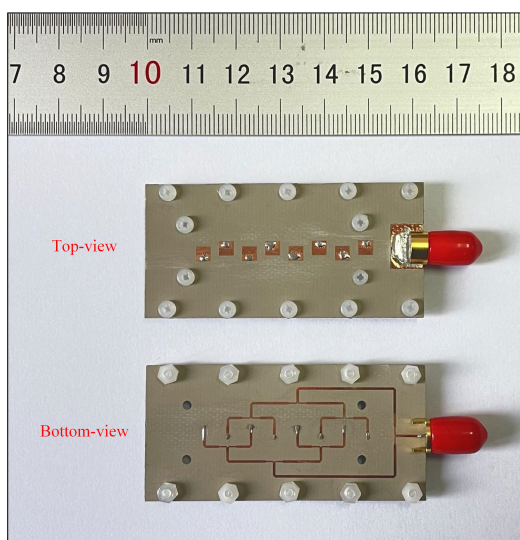


FIGURE 15. The photographs of the fabricated prototype.

IV. EXPERIMENT

A prototype of the proposed 8-unit wide-beam array antenna is fabricated to verify the design concept. Both the coupled-mode microstrip unit and the 1-8 feeding network are based on a Taconic RF-35 substrate with a dielectric constant of 3.5, a loss tangent of 0.003 and a thickness of 0.25 mm.

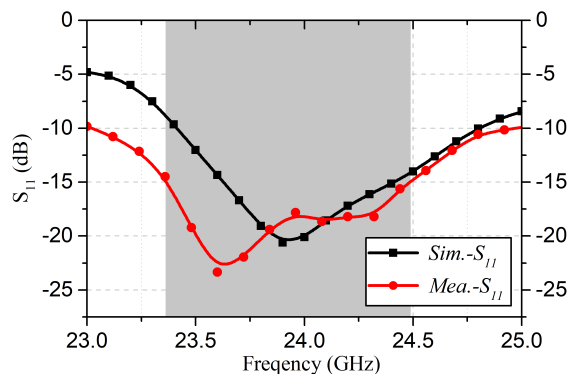


FIGURE 16. Simulated and measured S₁₁ of the fabricated prototype.

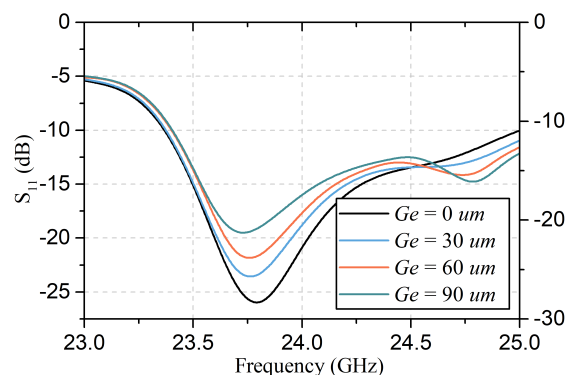


FIGURE 17. The effect of gap error on the reflection coefficient.

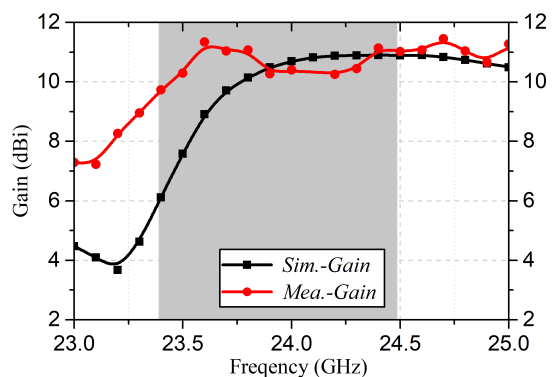


FIGURE 18. Simulated and measured gain of the fabricated prototype.

The two substrates are assembled together by reflow soldering process. The photograph of the wide-beam antenna prototype is shown in Fig. 15. It can be noticed that a 50-Ω SMA connector is soldered as the test port.

The measured reflection coefficients are compared with simulated results in Fig.16. Due to assembly errors, the measured working frequency band is slightly offset to the low frequency end. Based on the standard of $|S_{11}| < -10$ dB, the simulated results show impedance bandwidth of 5.8% (23.4 - 24.8 GHz) and the measured results shows a wider bandwidth. The difference between the simulated S₁₁ and

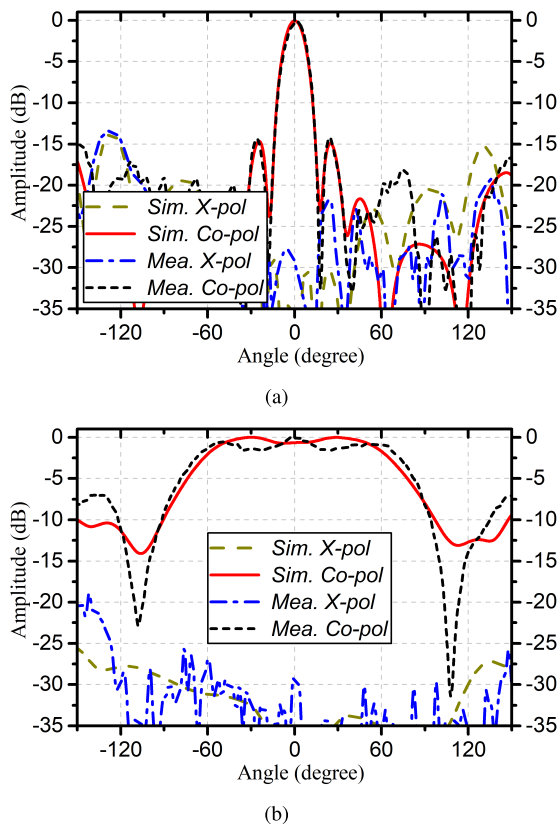


FIGURE 19. Simulated and measured radiation patterns of the wide-beam prototype. (a) H-plane and (b) E-plane.

measured one can be attributed to the fabrication error. The limited experimental conditions may leave an air gap between the two plates. The effect of the gap error is simulated and shown in Fig. 17. The existence of the air gap makes the antenna have a better impedance bandwidth and the dual-mode resonance characteristic is also clearer, which just coincides with the measured result (Fig.16). At the same time, the fabrication error also slightly shifts the working frequency band to the low frequency end. The measured antenna gain shows the same offset trend like the S_{11} (Fig. 18). In general, in the operating frequency band, the measured antenna gain is over 10 dBi and the fluctuation is less than 1.5 dB, which corresponds to a decent total antenna efficiency of about 0.7.

Fig. 19 shows the comparison of the simulated and measured normalized radiation patterns. Due to the frequency deviation, the simulated radiation patterns at 24 GHz are chosen for representative, and the corresponding measured patterns are selected at 23.7 GHz. Due to the symmetry characteristics of the unit H-plane radiation, the H-plane radiation patterns show typical narrow beam characteristics and the first side lobe is approximately -14 dB. The measured E-plane radiation patterns again verify the wide-beam design. The E-plane HPBW is over 140° , and the excellent wide-beam performance is suitable for automotive radar application. The obvious flat top feature of the E-plane patterns is also noteworthy even when the 1.5-dB beamwidth

is over 100° . The cross-polarization levels in both E-plane and H-plane are less than -25 dB. Hence the special flat top radiation pattern feature with good decent cross-polarization suppression performance gives this design more possible application scenarios, such as wide-angle scanning phased array application. Due to the parallel feeding scheme in this prototype, the footprint of the feeding network has a relatively large width, which limits its application in the array. However, this shortcoming can be achieved by adopting a multi-layer process or using a more compact series feeding network.

V. CONCLUSION

A novel wide-beam array antenna based on coupled-mode microstrip unit is proposed for automotive radar applications. The coupled-mode technology can achieve the inclined radiation beam. Arranging the array elements alternately and exciting with opposite phases can make the alternately offset unit radiation beams point to two sides of the array. Hence, wide-beam radiation can be realized in the direction perpendicular to the array. Meanwhile, the array feature can also maintain adequate antenna gain. This type of wide-beam one-dimensional array is very suitable for automotive radar applications, so an 8-unit prototype working at 24 GHz is designed and fabricated. Measured results show that the special design scheme extended the horizontal-plane HPBW to 140° with an antenna gain of approximately 10.5 dBi.

REFERENCES

- [1] J. Hatch, A. Topak, R. Schnabel, T. Zwick, R. Weigel, and C. Waldschmidt, "Millimeter-wave technology for automotive radar sensors in the 77 GHz frequency band," *IEEE Trans. Microw. Theory Techn.*, vol. 60, no. 3, pp. 845–860, Mar. 2012.
- [2] S. M. Patole, M. Torlak, D. Wang, and M. Ali, "Automotive radars: A review of signal processing techniques," *IEEE Signal Process. Mag.*, vol. 34, no. 2, pp. 22–35, Mar. 2017.
- [3] O. Khan, J. Meyer, K. Baur, S. Arafat, and C. Waldschmidt, "Hybrid thin film multilayer antenna for automotive radar at 77 GHz," in *Proc. 12th Eur. Conf. Antennas Propag. (EuCAP)*, Apr. 2018, pp. 1–5.
- [4] W. Wei and X. Wang, "A 77 GHz series fed weighted antenna arrays with suppressed sidelobes in E- and H-plane," *Prog. Electromagn. Res.*, vol. 72, pp. 23–28, Jan. 2018.
- [5] S. Yasini, K. Mohammadpour-Aghdam, and M. Mohammad-Taheri, "Low-cost comb-line-fed microstrip antenna arrays with low sidelobe level for 77 GHz automotive radar applications," *Prog. Electromagn. Res. M*, vol. 94, pp. 179–187, Jul. 2020.
- [6] A. Kuriyama, H. Nagaishi, H. Kuroda, and K. Takano, "A high efficiency antenna with horn and lens for 77 GHz automotive long range radar," in *Proc. 46th Eur. Microw. Conf. (EuMC)*, Oct. 2016, pp. 378–381.
- [7] S. Yoo, Y. Milyakh, H. Kim, C. Hong, and H. Choo, "Patch array antenna using a dual coupled feeding structure for 79 GHz automotive radar applications," *IEEE Antennas Wireless Propag. Lett.*, vol. 19, no. 4, pp. 676–679, Apr. 2020.
- [8] N. Wang, P. Gao, W. Zhao, and X. Wang, "The design of 77 GHz microstrip antenna array applied to automotive anti-collision radar antenna," in *Proc. IEEE Asia-Pacific Microw. Conf. (APMC)*, Dec. 2019, pp. 1238–1240.
- [9] J. Lee, J. M. Lee, and K. C. Hwang, "Series feeding rectangular microstrip patch array antenna for 77 GHz automotive radar," in *Proc. Int. Symp. Antennas Propag. (ISAP)*, Nov. 2017, pp. 1–2.
- [10] Y.-B. Kim, H.-J. Dong, K.-S. Kim, and H. L. Lee, "Compact planar multipole antenna for scalable wide beamwidth and bandwidth characteristics," *IEEE Trans. Antennas Propag.*, vol. 68, no. 5, pp. 3433–3442, May 2020.
- [11] Y.-B. Kim, S. Lim, and H. L. Lee, "Electrically conformal antenna array with planar multipole structure for 2-D wide angle beam steering," *IEEE Access*, vol. 8, pp. 157261–157269, 2020.

- [12] Z. Yi, R. Zhange, B. Xu, Y. Chen, L. Zhu, F. Li, G. Yang, and Y. Luo, "A wide-angle beam scanning antenna in E-plane for K-band radar sensor," *IEEE Access*, vol. 7, pp. 171684–171690, 2019.
- [13] C.-M. Liu, S.-Q. Xiao, H.-L. Tu, and Z. Ding, "Wide-angle scanning low profile phased array antenna based on a novel magnetic dipole," *IEEE Trans. Antennas Propag.*, vol. 65, no. 3, pp. 1151–1162, Mar. 2017.
- [14] C.-M. Liu, S. Q. Xiao, and X.-L. Zhang, "A compact, low-profile wire antenna applied to wide-angle scanning phased array," *IEEE Antennas Wireless Propag. Lett.*, vol. 17, no. 3, pp. 389–392, Mar. 2018.
- [15] N.-W. Liu, L. Zhu, Z.-X. Liu, and Y. Liu, "Dual-band single-layer microstrip patch antenna with enhanced bandwidth and beamwidth based on reshaped multiresonant modes," *IEEE Trans. Antennas Propag.*, vol. 67, no. 11, pp. 7127–7132, Nov. 2019.
- [16] C.-A. Yu, E. S. Li, H. Jin, Y. Cao, G.-R. Su, W. Che, and K.-S. Chin, "24 GHz horizontally polarized automotive antenna arrays with wide fan beam and high gain," *IEEE Trans. Antennas Propag.*, vol. 67, no. 2, pp. 892–904, Nov. 2018.
- [17] G.-R. Su, E. S. Li, T.-W. Kuo, H. Jin, Y.-C. Chiang, and K.-S. Chin, "79-GHz wide-beam microstrip patch antenna and antenna array for millimeter-wave applications," *IEEE Access*, vol. 8, pp. 200823–200833, 2020.
- [18] H. Tian, K. Dhvaj, L. J. Jiang, and T. Itoh, "Beam scanning realized by coupled modes in a single-patch antenna," *IEEE Antennas Wireless Propag. Lett.*, vol. 17, no. 6, pp. 1077–1080, Jun. 2018.
- [19] H. Tian, L. Jiang, and T. Itoh, "Compact endfire coupled-mode patch antenna with vertical polarization," *IEEE Trans. Antennas Propag.*, vol. 67, no. 9, pp. 5885–5891, Sep. 2019.
- [20] E. Guo, J. Liu, and Y. Long, "A mode-superposed microstrip patch antenna and its Yagi array with high front-to-back ratio," *IEEE Trans. Antennas Propag.*, vol. 65, no. 12, pp. 7328–7333, Dec. 2017.



XINYAN YANG is currently pursuing the B.S. degree with the Glasgow College, University of Electronic Science and Technology of China (UESTC). Her research interest includes automotive radar antennas.



XIANFENG LIU received the B.S. and M.S. degrees in electromagnetic field and microwave technique from the University of Electronic Science and Technology of China, Chengdu, China, in 1998 and 2001, respectively. Her current research interests include electromagnetic theories and computations, and antenna theories and designs.

• • •